ACS APPLIED MATERIALS & INTERFACES

Research Article

www.acsami.org

Engineering Natural Materials as Surface-Enhanced Raman Spectroscopy Substrates for In situ Molecular Sensing

Xiaojuan Liu, Chenghua Zong, Kelong Ai, Wenhui He, and Lehui Lu*

State Key Laboratory of Electroanalytical Chemistry, Changchun Institute of Applied Chemistry, Chinese Academy of Sciences, 5625 Renmin Street, Changchun 130022, P. R. China

Supporting Information

ABSTRACT: Surface-enhanced Raman spectroscopy (SERS) is a powerful analytical tool. However, its applications for in situ detection of target molecules presented on diverse material surfaces have been hindered by difficulties in rapid fabricating SERS-active substrates on the surfaces of these materials through a simple, low-cost, and portable approach. Here, we demonstrate our attempt to address this issue by developing a facile and versatile method capable of in situ generating silver nanoparticle film (SNF) on the surfaces of both artificial and natural materials in a simple, cheap, practical, and disposable manner. Taking advantage of the high SERS enhancement ability of the prepared SNF, the proposed strategy can be used for in situ inspecting herbicide and pesticide residues on vegetables, as well as the abuse of antiseptic in aquaculture industry. Therefore, it opens new avenues for advancing the application prospects of SERS technique in the fields of food safety, drug security, as well as environment monitoring.

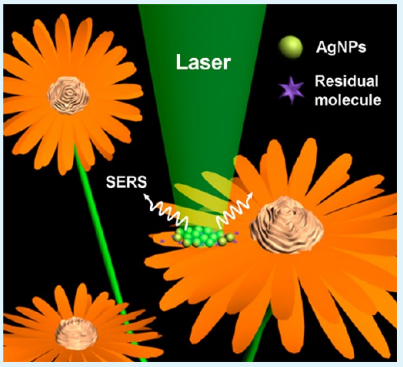

KEYWORDS: *surface-enhanced Raman spectroscopy, silver nanostructures, in situ synthesis, natural material, molecular sensing*

1. INTRODUCTION

Surface-enhanced Raman spectroscopy (SERS) as a powerful analytical tool is ideal for identifying and detecting specific targets, because of its ability to provide unique vibrational signatures of analytes associated with chemical and structural information.[1,2] Over the past several decades, tremendous efforts have been made in the design of high-performance SERS-active substrates for detecting particular analytes.[3−9] These sensing applications have been generally carried out by immersing the substrates in the solution of target molecules or directly adding the analytes onto their surfaces.[10−15] Therefore, how to in situ detect and identify analytes presented on diverse material surfaces is one of the major issues that hamper the wider application of SERS technique beyond the fundamental studies. In fact, there is an urgent requirement for expanding SERS technique to nontraditional but important surface analysis, such as the rapid in situ detection and identification of drug abuse,[16,17] herbicide/pesticide residues on agricultural products,[18,19] as well as marine toxins in food[20] and so on.[21−23]

To achieve such applications, it is necessary to develop a general method that is able to engineer metal nanostructures onto the surfaces of various supporting materials. Attempts to develop such method have been focused on noble metal nanopartilces (NPs), which are basic building blocks for fabrication of SERS substrates facilitating analytical applications.[24−28] Up to now, there have been enormous efforts and success in the preparation of metal NPs with desired sizes, shapes, as well as surface properties for providing large SERS signal enhancement and enabling them to be used in many important sensing applications.[29−34] For example, Au nanorods have been adsorbed onto filter paper for SERS detection of analytes by swabbing the surface under investigation.[25] AuNPs cluster arrays created by the template-guided self-assembly strategy have been used for the discrimination of bacteria species.[32] Shape-tunable Ag nanoplates in alumina sol have been directly used for sensing target molecules, which is performed by mixing them with analytes and then dropcasting on support materials for evaporation of solvent to form gel like solid and facilitate SERS detection.[33] Recently, Ag nanostructures generated by the laser-direct-writing technique have also been demonstrated to be active SERS substrates.[34] In addition to these immobilized metal NPs, metal colloidal NPs and their aggregates are also excellent SERS substrates available for analytical applications. More importantly, they are possible to be drop-cast onto various surfaces for realizing in situ detection of target molecules.[18,19,35,36] However, the main problems with these metal colloidal NPs are their poor stability and reproducibility owing to the easy oxidation or sulfuration of metal NPs (especially AgNPs) and the difficulty to control their aggregation, respectively.[37] In this regard, individual metal NPs with high stability and SERS activity are more attractive for probing target molecules on surfaces by using the strategy of drop casting. For example, gold NPs with ultrathin shell of silica have been successfully applied onto diverse material surfaces for in situ sensing applications.[18] Despite these amazing advances, the practical applications of SERS technique for in situ sensing

Received: August 20, 2012
Accepted: November 21, 2012
Published: November 21, 2012

   dx.doi.org/10.1021/am302376q | ACS Appl. Mater. Interfaces 2012, 4, 6599−6608

Scheme 1. Illustration of the Typical Procedure of the Modified Tollens Process for In situ Reducing Ag Precursor Solution into AgNPs on Petal Surface

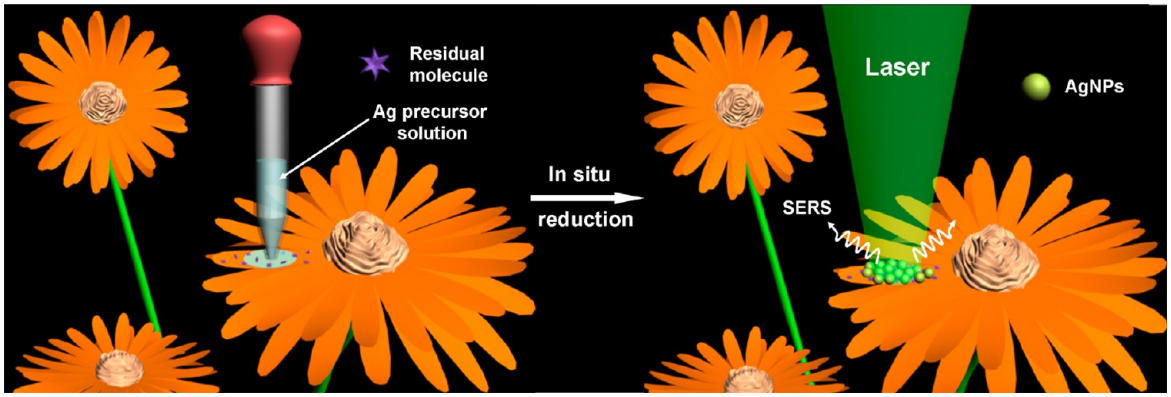

have been still restricted by some problems including the uniform distribution of the metal NPs on the entire surfaces, especially hydrophobic ones, and engineering the NPs to the morphologies inherited from the supporting materials.

With this in mind, we proposed a novel strategy, which offered opportunities to circumvent these problems. This strategy relied on in situ generation of silver nanoparticle film (SNF) on the surfaces of desired materials by using a modified Tollens process (Scheme 1).[38] Several features of such a strategy make it particularly attractive for in situ detection and identification of analytes presented on diverse material surfaces: (1) the modified Tollens process is simple and convenient; (2) no capping agent is needed and no residual reducing agent is left during the fabrication process; (3) the original silver precursor solution used in the process is stable for months under ambient conditions;[38] (4) this method enables in situ formation of SNF on the surfaces of almost any types of materials. The proof-of-concept experiments demonstrated that this strategy could be used for inspecting herbicide and pesticide residues on vegetables, as well as the abuse of antiseptic in aquaculture industry.

2. EXPERIMENTAL SECTION

Materials. All chemical regents and solvents were obtained from commercial suppliers and used without further purification. Ammonium hydroxide and 4-aminothiophenol (ATP) were purchased from Sigma-Aldrich. Silver acetate, formic acid, and ethanol were obtained from Beijing Chemical Reagent Co. Crystal violet (CV), amaranth, phosphorus triphenyl (PPh_3), malachite green (MG), paraquat, and fenthion were purchased from Aladdin. Deionized water (resistance >18.2 MΩ cm) was used in all reactions. The textiles and plastic were cut from commercial available cloth and plastic bags, respectively. The glass materials are common microscopy slides. The paper used in this study is a common laboratory cellulose filter paper with the pore sizes of ~0.22 μm. All of these artificial supporting materials were cut into pieces with dimensions of 1 cm × 1 cm. The flowers and other natural materials were obtained from flower shop and supermarket, respectively. These materials were cut into pieces of 0.7 cm × 0.7 cm, because of their small sizes and irregular shapes.

Fabrication of Silver Precursor Solution. The silver precursor solution was synthesized as previously described.[38] Briefly, 1 g of silver acetate was dissolved into 2.5 mL of aqueous ammonium hydroxide under vigorous stirring at room temperature. Then, formic acid (0.2 mL) was titrated into the solution. Subsequently, the solution was centrifugated to remove the large Ag particles, whereas the supernatant clear solution was collected and served as the reactive Ag precursor solution. This solution was defined as the original Ag precursor solution and the concentration of silver ions in the solution was about 2 M. In some cases, ethanol diluted Ag precursor solution was used, which was prepared by mixing the original Ag precursor solution with ethanol (v/v = 1:4). Thus, the concentration of silver ions was about 0.4 M in the diluted solution.

Preparation of SERS Substrates on Various Materials and SERS Sensing. For textile and filter paper, they were directly wetted by immersing into the original Ag precursor solution. The adsorbed Ag precursor solution was then reduced into AgNPs by heating at 60 °C until nearly dry. For other supporting materials, a drop of Ag precursor solution was placed onto the materials and heated at 60 °C to induce the formation of AgNPs. Particularly, 10 μL different concentrations of Ag precursor solution were applied on glass slides, whereas different volumes of ethanol diluted Ag precursor solution were dropped onto the surfaces of other materials (plastic pieces, petals, fish scales, and so on). To evaluate SERS performance, modification of ATP molecules on AgNPs-coated SERS substrates was preformed by incubation the substrates in 1×10^{-5} M ATP ethanol solution for 1 h, followed by rinsing with ethanol and drying in air. For sensing CV, amaranth, and PPh_3 molecules, AgNPs decorated textiles were soaked into their aqueous or ethanol solution for 1 h, then rinsing and drying in air. The detection of MG, paraquat, and fenthion residues was carried out by dropping their solutions onto the fish scales and vegetables before the deposition of AgNPs, respectively.

Fabrication of Ag Nanoislands by Using the Normal Tollens Process. In the control experiment, Ag nanoislands were deposited onto different material surfaces by using the normal Tollens process as previously reported.[39] In brief, 1.5 mL solution of 5% NaOH was added to a freshly prepared 0.05 M $AgNO_3$ (45 mL) solution. Subsequently, ammomium hydroxide was added drop by drop until the initially formed brown precipitate was dissolved. Then, the solution was cooled to 5 °C in an ice bath and a solution of 0.3 M glucose (11 mL) was added to form the Tollens' solution, followed by placing textiles, plastic pieces, and piranha solution treated glass slides into the solution for 10 min.

Characterization. Scanning electron microscope (SEM) images were taken using a FEI/Philips XL30 ESEM FEG field-emission scanning electron microscope. Energy-dispersive X-ray spectra (EDS) were collected on the FEI/Philips XL30 ESEM FEG equipped with an EDAX detector. X-ray photoelectron spectroscopy (XPS) measurement was performed on an ESCALAB-MKII 250 photoelectron spectrometer with Al KR X-ray radiation as the X-ray source for excitation. XRD data were measured on a D/Max 2500 V/PC X-ray diffractometer with a Cu Kα X-ray radiation source. Raman spectra were recorded with a Renishaw 2000 equipped by an Ar ion laser giving the excitation line of 514.5 nm and an air-cooling charge-coupled device (CCD) as the detector. The laser beam was focused on a spot with a diameter of approximately 1 μm using 25% laser power (10 mW at 100%). The data acquisition time was 10 s for one accumulation. The Raman band of a silicon wafer at 520 cm^{-1} was used to calibrate the spectrometer.

3. RESULTS AND DISCUSSION

Method for In situ Formation of Silver Nanoparticle Film (SNF). To apply SERS for molecular sensing purpose, the strategy for in situ fabrication of SNF should be operationally simple, convenient, and robust. Fortunately, the widely used Tollens process has guided us in the formation of an approach to achieve this purpose. Tollens process has been employed for many decades in the electroless deposition of silver to generate reflective mirrors on the surface of solid supports.[40−44] The fundamental reaction involves in the process can be simplified as follows.[45]

$$Ag(NH_3)_2^+(aq) + RCHO(aq) \rightarrow Ag(s) + RCO_2H(aq) \quad (1)$$

The Ag planting solution used in this process can be easily prepared by following the recipes outlined in a book.[40] However, the fast reduction of $[Ag(NH_3)_2]^+$ ions, which occurs as soon as the aldehydes or reducing sugars is added, makes it have a short shelf life and must be used quickly. To overcome this problem, we adopted a modified Tollens process, in which silver acetate in place of silver nitrate was used as silver precursor and formic acid was employed as a reduction agent. The inherent advantages of this modified Tollens process have been discussed in previous work.[38] It should be noted that the silver precursor solution is nonexplosive and stable for months when stored in an opaque and sealed vial under room temperature. As the solution dries under proper temperature, the formation of SNF occurs as follow.[38]

$$2Ag(NH_3)_2CH_3CO_2(aq) + HCO_2NH_4(aq) \xrightarrow{\Delta} 2Ag(s) + 5NH_3\uparrow + 2CH_3CO_2H\uparrow + CO_2\uparrow \quad (2)$$

In this process, temperature is a key factor determining the evaporation rate of the solvent and the formation of SNF. Therefore, it is necessary to optimize this condition. Figure S1A in the Supporting Information compares the SERS intensities obtained from the samples prepared under different temperatures by using 4-aminothiophenol (ATP) as probe molecule. Obviously, as the preparation temperature increases from 20 to 60 °C, the average SERS signal intensities increase and reach the highest intensities at 60 °C. But further increasing the temperature leads to a dramatic decrease of the SERS signal intensities (see Figure S1B in the Supporting Information). This observation can be understood by comparing the scanning electron microscopy (SEM) images of the samples prepared under different temperatures. As shown in Figure S2A−F in the Supporting information, the samples prepared under relatively low temperatures (≤60 °C) display two striking features: One is the uniform distribution of the fabricated silver nanoparticles (AgNPs); another is that increasing the preparation temperature tends to increase the coverage density of AgNPs. This increased coverage density, which is supposed to deliver a higher density of 'hot-spots', is probably responsible for the increased SERS signal intensities. In contrast, the extremely weak SERS signals observed from the samples prepared under high temperatures are likely caused by the coarsening of the metallic nanostructures and the formation of big blocks (see Figure S2G, H in the Supporting Information). In addition, it should be noted that the low coverage density formed at temperatures below 60 °C may arise from the fact that silver acetate can not be completely reduced to AgNPs under low temperature. This is deduced from the X-ray diffraction (XRD) and Raman spectroscopy. As shown in Figure S3A in the Supporting Information, both silver and silver acetate peaks were observed from the samples prepared by drying at 20 °C, whereas only silver peaks were observed from that of 60 and 90 °C. Similarly, the Raman background spectra (Figure S3B in the Supporting Information) also clearly show the characteristic peaks of silver acetate for the samples fabricated at 20 °C. Notably, these peaks disappear for the samples prepared at 60 and 90 °C. All these results indicate the presence of silver acetate in the samples dried at 20 °C and the absence of this substance upon heating at 60 °C. Besides, the SNF prepared at 60 °C were further characterized by energy-dispersive X-ray spectrometry (EDS) and X-ray photoelectron spectroscopy (XPS). The EDS spectrum, which has been taken from the sample on silicon wafer, reveals that only the element of Ag is left after drying Ag precursor solution at 60 °C (see Figure S3C in the Supporting Information). Furthermore, the high-resolution XPS spectrum of the Ag 3d region shows two obvious peaks at binding energy of 368.3 eV for Ag $3d_{5/2}$ state and 374.3 eV for the Ag $3d_{3/2}$ state (see Figure S3D in the Supporting Information), which correspond to the Ag^0 state.[46]

Versatility of the Method. In our method, when the samples are drying at 60 °C, the evaporation of solvent and the formation of AgNPs take place at the same time, which make the process very convenient for in situ generating SNF on material surfaces. In principle, the Ag precursor solution can be applied onto an arbitrary surface. Thus, we speculated that the proposed method may be generalized to produce SNF on diverse materials. To demonstrate it, we chose different types of artificial materials as model, including infiltrative materials with irregular surfaces and impermeable materials with their surfaces either hydrophilic or hydrophobic.

First, the widely used textile and paper as two kinds of representative infiltrative materials was used to demonstrate the versatility of the method due to their excellent properties, such as flexibility, low price and density, as well as the ability of absorbing water and other liquid. The in situ growth of SNF on their surfaces was carried out by dipping them into the original Ag precursor solution for a while and then drying them at 60 °C. The formation of SNF is evidenced by the SEM images, which reveal that AgNPs are uniformly and densely decorated on the surfaces of textile fiber (Figure 1A, B) and filter paper (Figure 1C, D) with their original structures unchanged.

A second demonstration of the versatility of the method was provided by using impermeable materials as model. Initially, glass slides were used because of their advantages of inexpensive, abundant, and disposable. The uniform growth of SNF across the entire glass surface (Figure 2A and Figure S4B in the Supporting Information) was achieved by casting 10 μL of aqueous Ag precursor solution onto the glass surface and then drying at 60 °C. It is worth noting that the superhydrophilicity of glass slide (see Figure S4A in the Supporting Information) makes it so the aqueous Ag precursor solution can cover the entire surface of the material, enabling the uniform distribution of the produced SNF. However, it is important to mention that, in nature, many material surfaces are hydrophobic, even superhydrophobic. Accordingly, it is still a challenge to homogeneously decorate their surfaces with AgNPs by the aqueous Ag precursor solution. To circumvent this problem, we diluted the original Ag precursor solution with ethanol. Ethanol was chosen here because it has a lower surface tension (22.1 mN m^{-1}) compared to that of water (72.8 mN m^{-1}) at room temperature.[47] As a result, the addition of ethanol

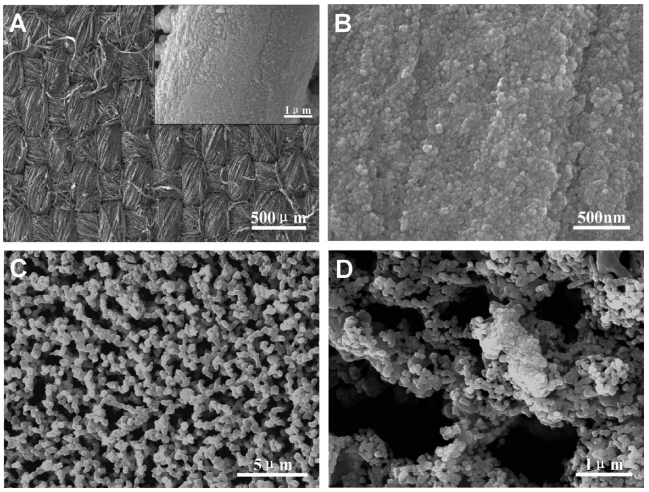

Figure 1. Low- and high-magnification SEM images of AgNPs decorated (A, B) textiles and (C, D) filter papers; inset, an image of a textile fiber.

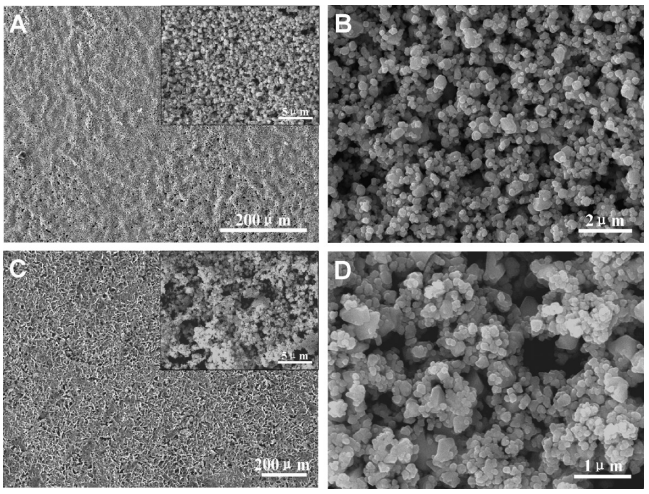

Figure 2. Low- and high-magnification SEM images of AgNPs decorated (A, B) glass slides and (C, D) plastic pieces.

would circumvent the difficulty of spreading Ag precursor solution onto the hydrophobic surfaces. To support this idea, plastic pieces from commercial available plastic bags were used as model. Figure 2C and Figure S4D in the Supporting Information provide clear evidence that AgNPs are evenly deposited on the surfaces of the plastic. Furthermore, the high magnification SEM image (Figure 2D) reveals that the SNF produced from the ethanol diluted Ag precursor solution is similar to that of the water diluted solution (Figure 2B). Particularly, the evaporation of the solvent molecules probably induces the formation of loose, fractal-like, porous structures, which are expected to be excellent candidates as SERS substrates because of their high surface areas and dense "hot-spots".[48,49] The average enhancement factor (EF) of the prepared SNF was estimated to be about 1.1×10^6 as detailed in the Supporting Information.

In the experiment, we found that the thickness of SNF can be controlled by varying the concentration or volume of Ag precursor solution. As infiltrative materials usually have irregular surfaces with their surface areas hard to define, in this case, we chose impermeable materials as examples. When kept other conditions unchanged, different concentrations of Ag precursor solution were placed onto the surfaces of the glass slides. Figure S5 in the Supporting Information and Figure 2A,B show the SNF formed at the silver ions concentrations ranging from 0.2 to 2 M. Obviously, as the concentration of silver ions increases, the produced AgNPs increases, leading to more densely loaded AgNPs on the surface. Furthermore, the effect of the amount of AgNPs on the SERS performance was investigated and displayed in Figure S6A in the Supporting Information. Evidently, increasing the concentration of silver ions increases the SERS intensity first, and afterward decreases it when the concentration is above 1 M. The relatively weak SERS enhancement at low concentration may be attributed to the sparse coverage of the glass slides with AgNPs (see Figure S5A, C in the Supporting Information), whereas the weak SERS enhancement at high concentration is likely due to the formation of large AgNPs (see Figure S5F in the Supporting Information). In addition to varying concentration, changing the volume of Ag precursor solution is also available for tuning the thickness of SNF. This strategy is more favorable for hydrophobic materials, owing to the fact that low concentration of ethanol diluted Ag precursor solution was used in this case. Thus, we drop-cast different volumes of ethanol diluted Ag precursor solution onto plastic pieces and dried them at 60 °C. The corresponding SERS performance in the presence of ATP molecules was evaluated and given in Figure S6B in the Supporting Information. Obviously, the change trend of the SERS intensity is similar to that of different concentrations.

Advantages of the Method over Normal Tollens Process. To clarify the advantages of the proposed method over normal Tollens process, we carried out a control experiment, in which normal Tollens process[39] was employed to deposit Ag nanoislands onto different material surfaces. In the case of glass slides, Ag nanoislands were uniformly deposited onto their surfaces (see Figure S7 in the Supporting Information) and formed mirror-like Ag films (see Figure S8A in the Supporting Information). Compared with the substrates prepared by using our modified Tollens process, this film gave lower SERS intensities under the same conditions (see Figure S9 in the Supporting Information, curves B−H). This observation is most likely from their different morphologies, and the loose, fractal-like, porous structures render the substrates prepared by our proposed method more excellent candidate for SERS sensing applications. Furthermore, very weak SERS signals were obtained from the plastic pieces and textiles that had been treated by the normal Tollens process (see Figure S9 in the Supporting Information, curves J, L). Also, poor SERS spectra were observed from the plastic pieces that had been immersed in the ethanol diluted Tollens' solution (see Figure S9 in the Supporting Information, curve N). These weak SERS signals are probably due to the failure of depositing Ag film onto these materials as evidenced in Figure S8B, C in the Supporting Information. Thus, the normal Tollens process is not a general method for deposition Ag film onto diverse material surfaces. Instead, our proposed method is a facile and versatile method that is capable of generating SNF on different types of material surfaces.

Extension of the Method to Natural Materials. Enlightened by the successful fabrication of SNF on different types of artificial materials, we further proceeded to modify the surfaces of natural materials with AgNPs through this method. Nature materials possess many sophisticated structures and topologies that cannot be typically replicated through

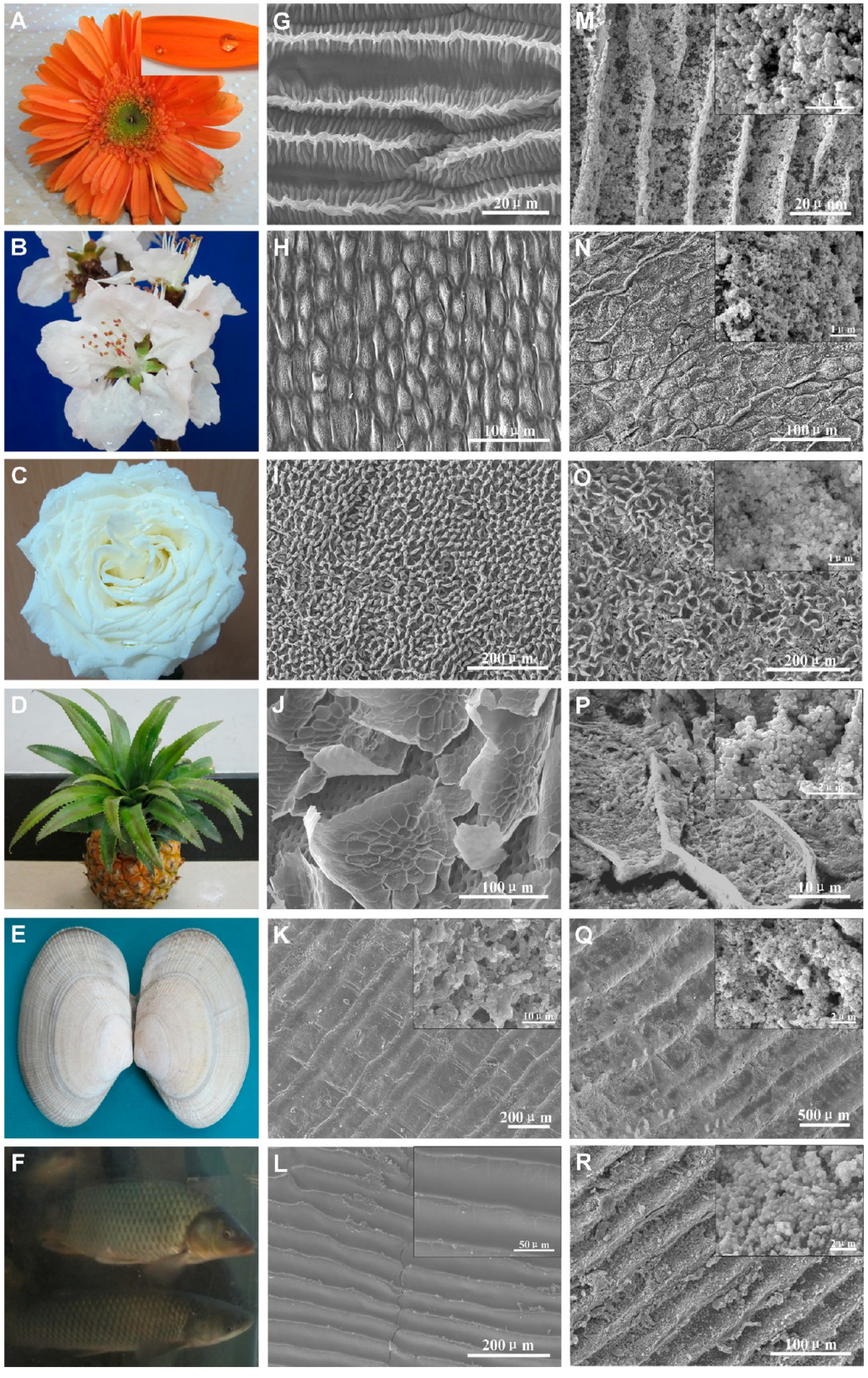

Figure 3. (A–F) digital photos of natural materials: marguerite, peach blossoms, rose, pineapple, clam shell, and fishes, respectively. Inset of A: photo of water droplets on the marguerite petal. (G–R) SEM images of these materials (G–L) before and (M–R) after decoration of AgNPs, respectively. The insets correspond to their high-magnification SEM images, respectively.

laboratory synthesis.[50] As a result, enormous efforts have been focused on the replication of diverse biological templates with noble metal as SERS substrates.[51−54] However, the original natural materials are commonly removed at last,[51−54] which is a hindrance for investigating the molecules presented on natural materials by using SERS technique. Therefore, the development

dx.doi.org/10.1021/am302376q | ACS Appl. Mater. Interfaces 2012, 4, 6599−6608

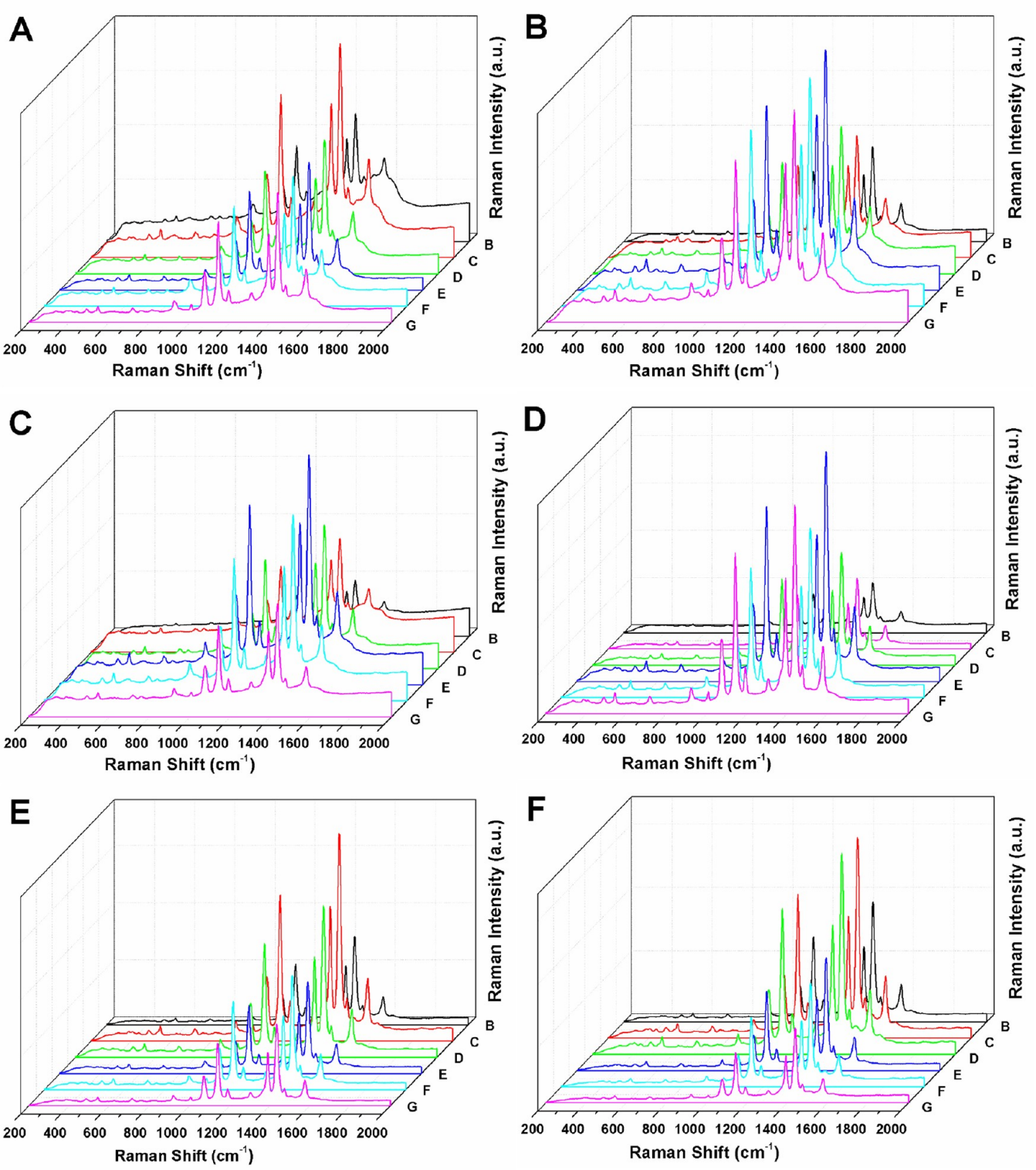

Figure 4. SERS spectra of ATP molecules on AgNPs decorated (A) marguerite petals, (B) peach blossom petals, (C) rose petals, (D) pineapple leaves, (E) clam shells, and (F) fish scales prepared under different volumes of ethanol diluted Ag precursor solution (0.4 M): curves B−G correspond to 5, 10, 15, 20, 25, and 30 μL, respectively. Each spectrum is the average of ten SERS spectra.

of simple and versatile method for in situ deposition of metal NPs on the surface of natural materials will significantly advance the prospects of SERS technique in the fields of identification natural materials and further understanding their fascinating properties, as well as mimicking their structures and properties for desired applications.

As a proof-of-concept experiment, six types of natural materials were used, including petals of marguerite, peach blossom, and rose, pineapple leaves, clam shells, and fish scales. Figure 3A−F gives the digital photos of these materials, while Figure 3 G-L and Figure 3 M-R present the SEM images of their morphologies before and after decoration of SNF,

respectively. Clearly, these materials all possess amazing microstructures, at the same time, exhibit different arrangements, orientations, and morphologies. For instance, the marguerite petals have parallel "main ridges" covered by perpendicular nanofolds, whereas the petals of peach blossom, and rose exhibit periodically and randomly distributed micropapillae, respectively. Interestingly, despite the different structures, the three petals are all hydrophobic. In contrast, the other three materials are hydrophilic. For pineapple leaves, it is likely that a substrate with many holes is covered by a lot of beautiful flower sheets. Besides, clam shells and fish scales possess ribbed textures. After the deposition of AgNPs, their surfaces are uniformly and densely covered by AgNPs, whereas their original morphologies are almost unchanged, except that the petals have shrunk a bit probably because of the loss of water. Moreover, the coverage density of the AgNPs can be controlled by varying the volume of Ag precursor solution (0.4 M, contains 80% ethanol) dropped on the surfaces. Increasing the volume of Ag precursor solution leads to a higher coverage density (see Figure S10 in the Supporting Information) along with increased SERS intensities (Figure 4A). But, when the amount of Ag precursor solution increases to a certain degree, the SERS intensities decline obviously (Figure 4A). The low SERS activities presumably arise from the formation of aggregates with large sizes and overlaying the original natural structures, which may result in a decrease in the surface area (see Figure S10E,F in the Supporting Information). The SERS spectra of the other five materials with different amount of AgNPs were also recorded (Figure 4B–F). Evidently, the average SERS intensities of ATP molecules on these materials follow the same trend as that of marguerite petals. However, the optimized amount of Ag precursor solution for these materials is distinctive, which is likely due to the differences in their microstructures and infiltration ability.

Applications. The observed results suggest that our method is flexile and versatile for producing SNF on surfaces of almost any types of materials, which can be further served as robust SERS substrates for carrying out molecular sensing with high sensitivity and specificity. One merit of this method is that the surface of the generated SNF is not passivated by any surfactant. Consequently, the SERS substrates prepared by this method would exhibit great potential for adsorbing molecules without the interference from their charge, which was demonstrated by using crystal violet (CV) with positive charge, amaranth with negative charge, and neutral phosphorus triphenyl (PPh_3) as model molecules. Their chemical structures are shown in Table S1 in the Supporting Information. In this case, the substrates supported on the textiles were used because of their good wettability, which made it very attractive for sensing the pollutions in water. As shown in Figure 5A, SERS signals of these molecules can be clearly observed and their characteristic peaks correspond well to the reported Raman spectra of CV,[55] amaranth,[56] and PPh_3,[57,58] respectively.

Another merit of this method is the capability of modifying AgNPs on the surfaces of many materials with a controlled coverage density, which renders our method available for in situ sensing molecules presented on various material surfaces (see section S2 in the Supporting Information). This will expand the potential applications of SERS technique in many fields, such as detection pesticide residues on vegetables, drug abuse in aquaculture industry, and so on. For example, malachite green (MG), which is a cationic triphenylmethane dye (see Table S1 in the Supporting Information), has been employed as a

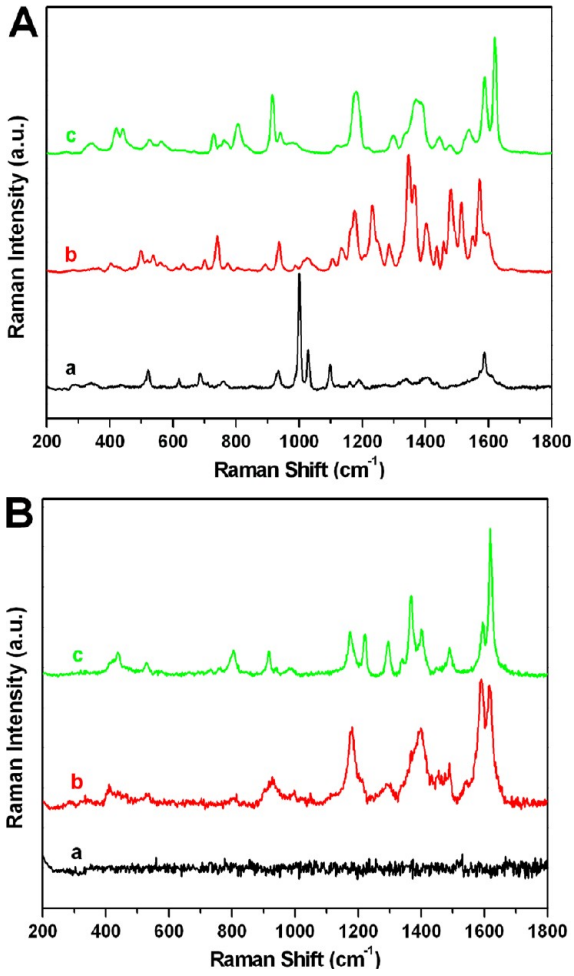

Figure 5. (A) SERS spectra of (a) PPh_3, (b) amaranth, and (c) CV on the textiles-based SERS substrates. (B) In situ detection of MG molecules on fish scales: (a, b) SERS spectra of fish scales in the (a) absence and (b) presence of 1×10^{-9} mol/cm^2 MG molecules; (c) Raman spectrum of solid MG.

fungicide and antiseptic in aquaculture industry. However, its use has been banned in several countries, because it is suspected to be genotoxic and carcinogenic.[59,60] Unfortunately, it is still illegally used by some people due to its low cost, availability, and efficacy. Consequently, a lot of effort has been directed toward the detection of trace amount of MG in water.[61−63] However, it is usually difficult for consumers to obtain the water samples directly from the market. An alternative strategy to solve this problem is to develop a new detection system that can monitor the residual MG on the aquatic products. To verify that our method is feasible for this practical application, Ag precursor solution was applied on the fish scales. Figure 5B depicts the SERS spectra of fish scales in the absence (curve a) and presence of MG molecules (curve b). Clearly, the observed prominent bands correspond well to the normal Raman spectrum of MG solid (curve c). The assignments of these peaks can be found in previous report.[64]

Furthermore, this approach can also be used for inspecting herbicide and pesticide residues on food, such as vegetables. In this study, we selected paraquat (1,1′-dimethyl-4,4′-bipyridinium) and fenthion (*O*,*O*-dimethyl-*O*-4-methylthio-m-tolyl phosphorothioate) as model molecules (see Table S1 in the Supporting Information) because of their widespread use in the

dx.doi.org/10.1021/am302376q | ACS Appl. Mater. Interfaces 2012, 4, 6599−6608

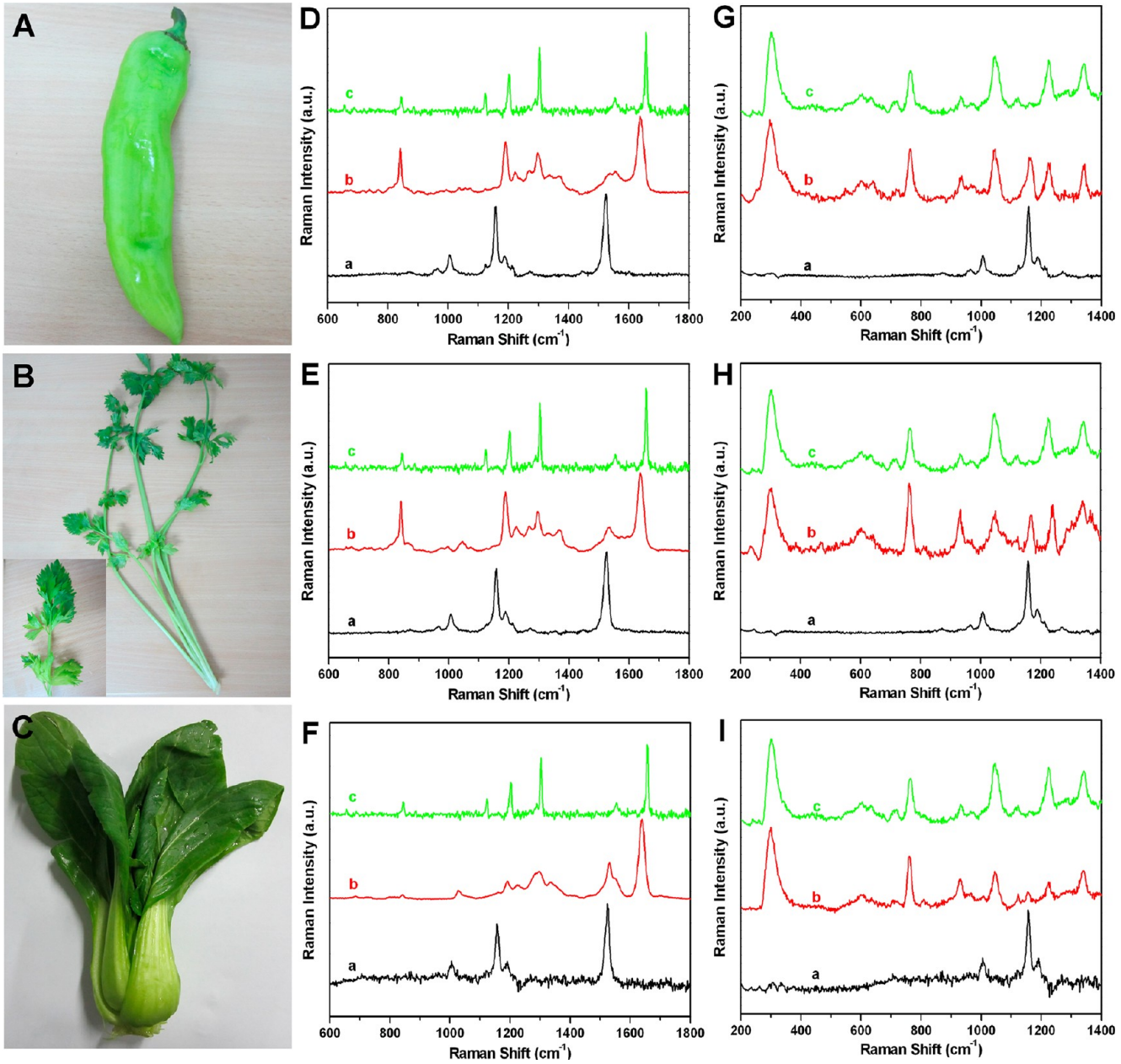

Figure 6. (A–C) digital photos of three vegetables: capsicum, celery, and cole, respectively. (D–F) In situ detection of paraquat on the three vegetables: SERS spectra of three (a) clean vegetables and (b) those contaminated by paraquat (1×10^{-8} mol/cm^2), respectively; (c) Raman spectra of solid paraquat. (G–I) In situ detection of fenthion on the three vegetables: (a, b) SERS spectra of three (a) clean vegetables and (b) those contaminated by fenthion (1×10^{-9} mol/cm^2), respectively; (c) SERS spectra of fenthion on the surface of AgNPs decorated glass slides.

agricultural practices as weed and insect killer, respectively. Paraquat is a nonselective fast-acting herbicide that has significant detrimental effects on human heart, liver, and brain tissue.[65] Fenthion is an organophosphate insecticide that is also a powerful inhibitor of cholinesterase enzymes.[66] As a result, they are all highly toxic to human health and the in situ analysis of their residues on agricultural products is very important for decreasing their threat to human/animal's health. Here, we demonstrated the successful detection of paraquat and fenthion on the surfaces of three vegetables (capsicum, celery, and cole) by using the modified Tollens process. Figure 6A–C illustrates the photographs of the three vegetables, whereas Figure 6D–I gives the typical Raman spectra collected from the clean or herbicide/pesticides contaminated vegetables. The Raman spectra of blank vegetables display two bands at about 1156 and 1525 cm^{-1}, which attribute to carotenoid molecules (Figure 6D–F, curve a).[18] In the herbicide contaminated samples, the characteristic vibrating bands of paraquat appear and even cover the weak signals of vegetables (Figure 6D–F, curve b). Furthermore, the observed bands match the Raman bands of paraquat solid, although there are slight shifts of some bands (Figure 6D–F, curve c). For example, the band of the paraquat solid at 1656 cm^{-1} that corresponds to C═N stretching[67] undergoes a downward shift; the band at 1203 cm^{-1} shifts to a lower frequency value. These shifts are likely attributed to interactions between paraquat and SERS substrate. Besides, the presence of fenthion on the three vegetables can also be similarly detected. As shown in Figure 6G–I curves b, the vibrating bands of fenthion and vegetables can be clearly distinguished.[68] In comparison with other

dx.doi.org/10.1021/am302376q | ACS Appl. Mater. Interfaces 2012, 4, 6599–6608

conventional sensing techniques,[63−66,68] the proposed method not only can result in comparable Raman enhancement but also is potentially practical for in situ inspecting drug and pesticide residues on various material surfaces.

4. CONCLUSIONS

In summary, we demonstrated a general and facile route for producing SERS active substrates by in situ growing SNF onto various artificial and natural materials, such as textile, plastic piece, petal, fish scale and so on. Furthermore, the coverage density of AgNPs can be controlled by varying the concentration or the volume of the Ag precursor solution. On the basis of the high SERS enhancement ability of the generated SNF, our method can be applied for rapid detection and identification of fungicide, herbicide, and pesticide residues on fish scales and vegetables, respectively. Therefore, our method exhibits great practical potentials for in situ inspecting food safety, drug security and environment pollutants. This will open new avenues for developing SERS technique into a simple, practical, disposable, and portable characterization tool for using in basic and applied research areas of natural sciences, industry, and even daily life.

■ ASSOCIATED CONTENT

Ⓢ Supporting Information

Further discussions on enhancement factor (EF) of SNF, optimization of SNF thickness for in situ sensing application, as well as supporting figures and table are available free of charge via the Internet at http://pubs.acs.org/.

■ AUTHOR INFORMATION

Corresponding Author

*Fax: (+86) 431-85262406. Tel: (+86) 431-85262418. E-mail: lehuilu@ciac.jl.cn.

Notes

The authors declare no competing financial interest.

■ ACKNOWLEDGMENTS

Financial support by the National Basic Research Program of China (973 Program; 2010CB933600), NSFC (20873138), and the "Hundred Talents Project" of Chinese Academy of Sciences is gratefully acknowledged.

■ REFERENCES

(1) Casadio, F.; Leona, M.; Lombardi, J. R.; Van Duyne, R. P. *Acc. Chem. Res.* **2010**, *43*, 782−791.
(2) Nie, S.; Emory, S. R. *Science* **1997**, *275*, 1102−1106.
(3) Lu, L. H.; Eychmüller, A. *Acc. Chem. Res.* **2008**, *41*, 244−253.
(4) Lin, X. M.; Cui, Y.; Xu, Y. H.; Ren, B.; Tian, Z. Q. *Anal. Bioanal. Chem.* **2009**, *394*, 1729−1745.
(5) Tan, E. Z.; Yin, P. G.; You, T. T.; Wang, H.; Guo, L. *ACS Appl. Mater. Interfaces* **2012**, *4*, 3432−3437.
(6) Zhao, X. M.; Zhang, B. H.; Ai, K. L.; Zhang, G.; Cao, L. Y.; Liu, X. J.; Sun, H. M.; Wang, H. S.; Lu, L. H. *J. Mater. Chem.* **2009**, *19*, 5547−5553.
(7) Yu, W. W.; White, I. M. *Anal. Chem.* **2010**, *82*, 9626−9630.
(8) Li, J. L.; Chen, L. X.; Lou, T. T.; Wang, Y. Q. *ACS Appl. Mater. Interfaces* **2011**, *3*, 3936−3941.
(9) Anderson, D. J.; Moskovits, M. A. *J. Phys. Chem. B* **2006**, *110*, 13722−13727.
(10) Cao, Y. W. C.; Jin, R. C.; Mirkin, C. A. *Science* **2002**, *297*, 1536−1540.
(11) Liu, T. Y.; Tsai, K. T.; Wang, H. H.; Chen, Y.; Chen, Y. H.; Chao, Y. C.; Chang, H. H.; Lin, C. H.; Wang, J. K.; Wang, Y. L. *Nat. Commun.* **2011**, *2*, 538.
(12) Huang, J. Y.; Zong, C.; Xu, L. J.; Cui, Y.; Ren, B. *Chem. Commun.* **2011**, *47*, 5738−5740.
(13) Zhang, B. H.; Wang, H. S.; Lu, L. H.; Ai, K. L.; Zhang, G.; Cheng, X. L. *Adv. Funct. Mater.* **2008**, *18*, 2348−2355.
(14) Yang, L. B.; Liu, H. L.; Wang, J.; Zhou, F.; Tian, Z. Q.; Liu, J. H. *Chem. Commun.* **2011**, *47*, 3583−3585.
(15) Liu, X. J.; Cao, L. Y.; Song, W.; Ai, K. L.; Lu, L. H. *ACS Appl. Mater. Interfaces* **2011**, *3*, 2944−2952.
(16) Frank, I.; Chetan, S.; Atanu, S.; Hermes, H.; Stuart, F. *Appl. Spectrosc.* **2011**, *65*, 1004−1008.
(17) Song, W.; Mao, Z.; Liu, X. J.; Lu, Y.; Li, Z. S.; Zhao, B.; Lu, L. H. *Nanoscale* **2012**, *4*, 2333−2338.
(18) Li, J. F.; Huang, Y. F.; Ding, Y.; Yang, Z. L.; Li, S. B.; Zhou, X. S.; Fan, F. R.; Zhang, W.; Zhou, Z. Y.; Wu, D. Y.; Ren, B.; Wang, Z. L.; Tian, Z. Q. *Nature* **2010**, *464*, 392−395.
(19) Liu, B. H.; Han, G. M.; Zhang, Z. P.; Liu, R. Y.; Jiang, C. L.; Wang, S. H.; Han, M. Y. *Anal. Chem.* **2012**, *84*, 255−261.
(20) Lin, W. C.; Jen, H. C.; Chen, C. L.; Hwang, D. F.; Chang, R.; Hwang, J. S.; Chiang, H. P. *Plasmonics* **2009**, *4*, 187−192.
(21) Brosseau, C. L.; Gambardella, A.; Casadio, F.; Grzywacz, C. M.; Wouters, J.; Van Duyne, R. P. *Anal. Chem.* **2009**, *81*, 3056−3062.
(22) Leona, M.; Lombardi, J. R. *J. Raman Spectrosc.* **2007**, *38*, 853−858.
(23) Jurasekova, Z.; Domingo, C.; Garcia-Ramos, J. V.; Sanchez-Cortes, S. *J. Raman Spectrosc.* **2008**, *39*, 1309−1312.
(24) Abalde-Cela, S.; Ho, S.; Rodríguez-González, B.; Duarte, M. A. C.; Álvarez-Puebla, R. A.; Liz-Marzán, L. M.; Kotov, N. A. *Angew. Chem., Int. Ed.* **2009**, *48*, 5326−5329.
(25) Lee, C. H.; Tian, L. M.; Singamaneni, S. *ACS Appl. Mater. Interfaces* **2010**, *2*, 3429−3435.
(26) Chang, S.; Combs, Z. A.; Gupta, M. K.; Davis, R.; Tsukruk, V. V. *ACS Appl. Mater. Interfaces* **2010**, *2*, 3333−3339.
(27) Guerrini, L.; Sanchez-Cortes, S.; Cruz, V. L.; Martinez, S.; Ristori, S.; Feis, A. *J. Raman Spectrosc.* **2011**, *42*, 980−985.
(28) Que, R. H.; Shao, M. W.; Zhuo, S. J.; Wen, C. Y.; Wang, S. D.; Lee, S. T. *Adv. Funct. Mater.* **2011**, *21*, 3337−3343.
(29) Mulvihill, M.; Tao, A.; Benjauthrit, K.; Arnold, J.; Yang, P. D. *Angew. Chem., Int. Ed.* **2008**, *47*, 6456−6460.
(30) Wang, J.; Kong, L. T.; Guo, Z.; Xu, J. Y.; Liu, J. H. *J. Mater. Chem.* **2010**, *20*, 5271−5279.
(31) Strickland, A. D.; Batt, C. A. *Anal. Chem.* **2009**, *81*, 2895−2903.
(32) Yan, B.; Thubagere, A.; Premasiri, W. R.; Ziegler, L. D.; Negro, L. D.; Reinhard, B. M. *ACS Nano* **2009**, *3*, 1190−1202.
(33) Jana, D.; Mandal, A.; De, G. *ACS Appl. Mater. Interfaces* **2012**, *4*, 3330−3334.
(34) Tseng, M. L.; Huang, Y. W.; Hsiao, M. K.; Huang, H. W.; Chen, H. M.; Chen, Y. L.; Chu, C. H.; Chu, N. N.; He, Y. J.; Chang, C. M.; Lin, W. C.; Huang, D. W.; Chiang, H. P.; Liu, R. S.; Sun, G.; Tsai, D. P. *ACS Nano* **2012**, *6*, 5190−5197.
(35) Li, J. F.; Ding, S. Y.; Yang, Z. L.; Bai, M. L.; Anema, J. R.; Wang, X.; Wang, A.; Wu, D. Y.; Ren, B.; Hou, S. M.; Wandlowski, T.; Tian, Z. Q. *J. Am. Chem. Soc.* **2011**, *133*, 15922−15925.
(36) Yang, D. H.; Xia, L. X.; Zhao, H. P.; Hu, X. H.; Liu, Y.; Li, J. S.; Wan, X. F. *Chem. Commun.* **2011**, *47*, 5873−5875.
(37) Tantra, R.; Brown, R. J. C.; Milton, M. J. T. *J. Raman Spectrosc.* **2007**, *38*, 1469−1479.
(38) Walker, S. B.; Lewis, J. A. *J. Am. Chem. Soc.* **2012**, *134*, 1419−1421.
(39) Ray, K.; Badugu, R.; Lakowicz, J. R. *J. Am. Chem. Soc.* **2006**, *128*, 8998−8999.
(40) Ingalls, A. G. In *Amateur Telescope Making*. Ingalls, A. G., Porter, R. W., Eds.; Scientific American Inc.: New York, 1981; Vol. *1*, p 101.
(41) Norrod, K. L.; Sudnik, L. M.; Rousell, D.; Rowlen, K. L. *Appl. Spectrosc.* **1997**, *51*, 994−1001.
(42) Leona, M.; Stenger, J.; Ferloni, E. *J. Raman Spectrosc.* **2006**, *37*, 981−992.

(43) Wang, H.; Chen, D.; Wei, Y.; Chang, Y.; Zhao, J. *Anal. Sci.* **2011**, *27*, 937−941.
(44) Šišková, K.; Bečička, O.; Mašek, V.; Šafářová, K.; Zbořil, R. *J. Raman Spectrosc.* **2012**, *43*, 689−691.
(45) Yin, Y. D.; Li, Z. Y.; Zhong, Z. Y.; Gates, B.; Xia, Y. N.; Venkateswaranc, S. *J. Mater. Chem.* **2002**, *12*, 522−527.
(46) Lu, Z.; Cheng, H.; Lo, M.; Chung, C. Y. *Adv. Funct. Mater.* **2007**, *17*, 3885−3896.
(47) Li, J.; Liang, G. Q.; Zhu, X. L.; Yang, S. *Adv. Funct. Mater.* in press, DOI: 10.1002/adfm.201200013.
(48) Tsai, D. P.; Kovacs, J.; Wang, Z.; Moskovits, M.; Shalaev, V. M.; Suh, J. S.; Botet, R. *Phys. Rev. Lett.* **1994**, *72*, 4149−4152.
(49) Safonov, V. P.; Shalaev, V. M.; Markel, V. A.; Danilova, Y. E.; Lepeshkin, N. N.; Kim, W.; Rautian, S. G.; Armstrong, R. L. *Phys. Rev. Lett.* **1998**, *80*, 1102−1105.
(50) Liu, K. S.; Jiang, L. *ACS Nano* **2011**, *5*, 6786−6790.
(51) Payne, E. K.; Rosi, N. L.; Xue, C.; Mirkin, C. A. *Angew. Chem., Int. Ed.* **2005**, *44*, 5064−5067.
(52) Tan, Y. W.; Gu, J. J.; Zang, X. N.; Xu, W.; Shi, K. C.; Xu, L. H.; Zhang, D. *Angew. Chem., Int. Ed.* **2011**, *50*, 8307−8311.
(53) Tan, Y. W.; Gu, J. J.; Xu, L. H.; Zang, X. N.; Liu, D. X.; Zhang, W.; Liu, Q. L.; Zhu, S. M.; Su, H. L.; Feng, C. L.; Fan, G. L.; Zhang, D. *Adv. Funct. Mater.* **2012**, *22*, 1578−1585.
(54) Yu, Y.; Addai-Mensah, J.; Losic, D. *Langmuir* **2010**, *26*, 14068−14072.
(55) Zhang, L.; Lang, X. Y.; Hirata, A.; Chen, M. W. *ACS Nano* **2011**, *5*, 4407−4413.
(56) Snehalatha, M.; Ravikumar, C.; Sekar, N.; Jayakumar, V. S.; Joe, I. H. *J. Raman Spectrosc.* **2008**, *39*, 928−936.
(57) Zimmermanna, F.; Wokaun, A. *Mol. Phys.* **1991**, *73*, 959−972.
(58) Song, Y. Y.; Butler, I. S.; Shaver, A. *Spectrochim. Acta, Part A* **2002**, *58*, 2581−2587.
(59) Bose, B.; Motiwale, L.; Rao, K.V. K. *Cancer Lett.* **2005**, *230*, 260−270.
(60) Stammati, A.; Nebbia, C.; Angelis, I. D.; Albo, A. G.; Carletti, M.; Rebecchi, C.; Zampaglioni, F.; Dacasto, M. *Toxicol. In Vitro* **2005**, *19*, 853−858.
(61) Han, B.; Choi, N.; Kim, K. H.; Lim, D. W.; Choo, J. *J. Phys. Chem. C* **2011**, *115*, 6290−6296.
(62) Wang, H. H.; Cheng, T. Y.; Sharma, P.; Chiang, F. Y.; Chiu, S. W. Y.; Wang, J. K.; Wang, Y. L. *Nanotechnology* **2011**, *22*, 385702.
(63) Lee, S.; Choi, J.; Chen, L.; Park, B.; Kyong, J. B.; Seong, G. H.; Choo, J.; Lee, Y.; Shin, K. H.; Lee, E. K.; Joo, S. W.; Lee, K. H. *Anal. Chim. Acta* **2007**, *590*, 139−144.
(64) Cecchini, M. P.; Hong, J.; Lim, C.; Choo, J.; Albrecht, T.; deMello, A. J.; Edel, J. B. *Anal. Chem.* **2011**, *83*, 3076−3081.
(65) Gao, R.; Choi, N.; Chang, S. I.; Kang, S. H.; Song, J. M.; Cho, S. I.; Lim, D. W.; Choo, J. *Anal. Chim. Acta* **2010**, *681*, 87−91.
(66) Guo, W.; Engelman, B. J.; Haywood, T. L.; Blok, N. B.; Beaudoin, D. S.; Obare, S. O. *Talanta* **2011**, *87*, 276−283.
(67) Tang, H. R.; Li, Q. Q.; Ren, Y. L.; Geng, J. P.; Cao, P.; Sui, T.; Wang, X.; Du, Y. P. *Chin. Chem. Lett.* **2011**, *22*, 1477−1480.
(68) Skoulika, S. G.; Georgiou, C. A.; Polissiou, M. G. *Appl. Spectrosc.* **1999**, *53*, 1470−1474.